

as LB films. This Account has described only those new reactions and applications that have been devised within the past few years, and it is certain that many more will be dreamed of in the years to follow.

We thank Prof. Abraham Clearfield and Dr. Howard Katz for communicating prior to publication results that are cited in this

Account. We also thank our co-workers, past and present, who have taken this project in many creative directions. This work has been supported by grants from the National Institutes of Health (GM43844), the National Science Foundation (CHE-8657729), and the Robert A. Welch Foundation. T.E.M. also thanks the Camille and Henry Dreyfus Foundation for support in the form of a Teacher-Scholar award.

## Vibrational Spectroscopy of High-Temperature, Dense Molecular Fluids by Coherent Anti-Stokes Raman Scattering

STEPHEN C. SCHMIDT\* and DAVID S. MOORE\*

Los Alamos National Laboratory, Los Alamos, New Mexico 87545

Received November 22, 1991 (Revised Manuscript Received May 11, 1992)

The behavior of liquids and dense fluids has been the subject of several previous Accounts.<sup>1-3</sup> In a dense fluid the short-range repulsive interparticle (or intermolecular for our studies) forces dominate and determine the structure and thermodynamic behavior of the fluid.<sup>1-4</sup> This dominance is especially true in materials subjected to shock waves or explosive detonations in which the densities may be two or more times the initial densities and temperatures may be several thousand degrees. The structure, thermodynamics, energy transfer, and chemical reactions of dense fluids have been described theoretically in terms of intermolecular (and intramolecular, for interactions within the molecule) potential functions and statistical mechanical treatments.<sup>1,3-13</sup> For liquids of not too high density, pairwise additive potential functions can be used. However, many-body effects necessitate corrections for the high-temperature dense fluids of interest in this Account.<sup>1,3,6</sup>

Experimental confirmation of these theoretical descriptions, especially for high-temperature dense fluids, has been obtained in several ways. First, these descriptions have been compared with the results of hydrodynamic/thermodynamic experiments such as shock Hugoniot measurements<sup>4,9</sup> or with numerical simulations, that is, computer experiments.<sup>5,8</sup> A shock Hugoniot is the locus of all pressure-volume end states attainable by a shock wave propagating into a particular initial pressure-volume state. The problem is that

macroscopic experiments such as shock Hugoniot measurements average over the microscopic (that is, molecular) aspects of the fluid and are, therefore, inadequate for a complete understanding of dense fluid behavior. Consequently, present models of dense fluids have been verified only to the extent that they agree with such bulk property measurements. A complete verification of these models requires more experimental data,<sup>3</sup> particularly from experiments that provide insight at the molecular level. In this Account, we describe an experiment, based on combining shock-compression techniques and nonlinear optical scattering methods, that was used to explore the microscopic aspects of dense fluid nitrogen, oxygen, and carbon monoxide. These simple diatomic molecules were chosen because initial results are easy to interpret and because these molecules are important in explosive applications.

### The Experiment

Spectroscopic measurements, when possible, can provide the desired microscopic level information. Recently, we have been able to probe some of the microscopic phenomenology of high-temperature dense fluids<sup>14,15</sup> using samples of liquid nitrogen, oxygen, and

Stephen C. Schmidt is a staff member in the Shock Wave Physics Group at the Los Alamos National Laboratory. He was born in Bay City, Michigan, March 1939, and received B.S. and M.S. degrees in aeronautical engineering from the University of Michigan. After several years of working in the aerospace industry, he obtained a Ph.D. in physics from the University of Denver. Prior to coming to Los Alamos, he was a faculty member in the Mechanical Engineering Department at Washington State University. His research interests include quantitative spectroscopy in condensed- and gas-phase systems and the behavior of dense fluids and explosives.

David S. Moore was born in Salt Lake City, Utah, on June 26, 1952. He received a B.S. degree in chemistry from the University of Utah in 1974 and a Ph.D. degree in physical chemistry from the University of Wisconsin-Madison in 1980. He joined Los Alamos National Laboratory in 1980 as a postdoctoral fellow and became a permanent staff member in 1981 and Section Leader in 1987. His main research interests are the study of shock-compressed molecular materials using optical spectroscopies, ultrafast chemical dynamics in condensed-phase materials, and development of field-deployable optical analytical instrumentation.

- (1) Chandler, D. *Acc. Chem. Res.* 1974, 7, 246-251.
- (2) Jonas, J. *Acc. Chem. Res.* 1983, 17, 74-81.
- (3) Alder, B. J.; Ceperley, D. M.; Pollock, E. L. *Acc. Chem. Res.* 1985, 18, 268-273.
- (4) Ross, M.; Ree, F. H. *J. Chem. Phys.* 1980, 73, 6146-6152.
- (5) Barker, J. A.; Henderson, D. *Rev. Mod. Phys.* 1976, 48, 587-671.
- (6) Ross, M. *J. Chem. Phys.* 1979, 71, 1567-1571.
- (7) Ree, F. H.; Winter, N. W. *J. Chem. Phys.* 1980, 73, 322-336.
- (8) Shaw, M. S.; Johnson, J. D.; Holian, B. L. *Phys. Rev. Lett.* 1983, 50, 1141-1144.
- (9) Johnson, J. D.; Shaw, M. S.; Holian, B. L. *J. Chem. Phys.* 1984, 80, 1279-1294.
- (10) Belak, J.; Eppers, R. D.; LeSar, R. *J. Chem. Phys.* 1988, 89, 1625-1633.
- (11) Oxtoby, D. W. *Annu. Rev. Phys. Chem.* 1981, 32, 77-101.
- (12) Blais, N. C.; Stine, J. R. *J. Chem. Phys.* 1990, 93, 7914-7922.
- (13) Brenner, D. W. In *Shock Compression of Condensed Matter-1991*; Schmidt, S. C., Dick, R. D., Forbes, J. W., Tasker, D. G., Eds.; North Holland: Amsterdam, in press.
- (14) Moore, D. S.; Schmidt, S. C.; Shaner, J. W. *Phys. Rev. Lett.* 1983, 50, 1819-1822.

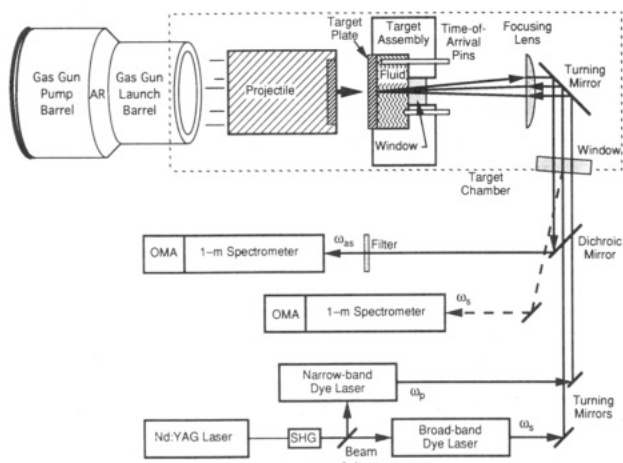


**Figure 1.** Schematic of the CARS experimental setup for shock-compressed materials. The fluid in the target is dynamically compressed by impact of the projectile from a two-stage gas gun. The output from a Nd:YAG laser pumps a narrow-band dye laser to provide the pump frequency and a broadband dye laser to provide a broad range of Stokes frequencies. The CARS signal is detected by an intensified photodiode array (OMA) gated on for 20 ns at the expected time of arrival of the signal. Two 1-m spectrometers are used, one to measure the CARS signal,  $\omega_{as}$ , produced in the sample and the other (in conjunction with a photodiode array) to measure the spectral profile of the broadband dye laser,  $\omega_s$ . AR denotes the accelerating reservoir of the gas gun, and SHG corresponds to second harmonic generation.

carbon monoxide shock-compressed to 2–3 times their initial density and several thousand degrees. Single-pulse, broadband, coherent, anti-Stokes Raman spectroscopy (CARS) was used to obtain the vibrational spectra of the high-temperature dense fluids.<sup>16–18</sup>

A complete experimental description has been given elsewhere.<sup>14,15</sup> Briefly, as shown in Figure 1, a projectile launched by a two-stage gas gun dynamically compresses a sample in a target. Our gas gun uses a powder charge to drive a piston in a barrel to compress a hydrogen working gas. The compressed hydrogen then accelerates a second, smaller projectile in a second barrel to velocities between 3 and 7 km s<sup>-1</sup>. The impact of this projectile on the target generates a strong shock wave that compresses the sample. The cryogenic target assembly used to condense and hold the liquid for these experiments consists of a highly-polished stainless steel target plate at the front and a lithium fluoride window at the rear. Impactor and target plate thicknesses were chosen, and electrical time-of-arrival pin assemblies were installed in the ~1.5 mm long liquid samples, so as to ensure that rarefaction waves from the rear and the side of the target would not compromise the one-dimensional character of the compression in the region observed optically. We calculated pressures, densities, and temperatures for the shock-compressed fluid using an effective spherical potential that has been shown to accurately reproduce both molecular dynamics simu-

lations with nonspherical potentials and experimental Hugoniot data.<sup>8,9</sup>

CARS<sup>19–24</sup> is a parametric process in which three waves, two at a pump frequency  $\omega_p$  and one at a Stokes frequency  $\omega_s$ , are mixed in a sample to produce a coherent beam at the anti-Stokes frequency  $\omega_{as} = 2\omega_p - \omega_s$ . The efficiency of this mixing is greatly enhanced if the frequency difference  $2\omega_p - \omega_s$  coincides with the frequency  $\omega_j$  of a Raman active mode of the sample and/or if  $\omega_p$ ,  $\omega_s$ , and/or  $\omega_{as}$  are tuned to electronic transitions of the scattering molecule.<sup>23,25,26</sup> The advantages of using CARS rather than spontaneous Raman scattering are that it provides a large scattering intensity, beamlike scattering rather than scattering into  $4\pi$  steradians, and the frequency  $\omega_{as}$  of the scattered signal greater than the initial laser frequencies at  $\omega_p$  and  $\omega_s$ . The latter feature mitigates the interference from possible sample fluorescence.

We obtained the pump frequency in the CARS process (Figure 1) by using a portion of the 5–10-ns frequency-doubled output of an injection-seeded, single-frequency Nd:YAG laser to pump a narrow-band, tunable dye laser. A broad range of Stokes frequencies was produced by a home-built, broadband dye laser pumped by the remaining Nd:YAG output. Flash lamp and Q-switch timing were provided by a photomultiplier tube/HeNe laser combination (not shown in Figure 1) activated by the projectile and the electrical time-of-arrival pins, respectively. The CARS signals produced in the sample were directed through a narrow-band filter monochromator and then dispersed by a 1-m spectrometer. To obtain multichannel detection of the CARS signal, we used an intensified photodiode array gated on for 20 ns at the expected arrival time of the CARS signal. Gating the detector on for only a short time eliminated any stray light produced by the gas gun. In addition, the broadband dye laser spectral profile was measured in each experiment by another 1-m spectrometer and photodiode array. The latter measurement was made to help achieve accurate data simulation.

Figures 2 and 3 show samples of the single-pulse, multichannel CARS spectra that were recorded. For experiments in which the shock wave in the target had not reached the window (see Figure 1), spectra corresponding to the solid curves in Figure 2 (top) and 3 were obtained. Figure 2 illustrates the results for a single-component sample such as nitrogen. Figure 3 represents spectra typical of mixtures, in this case 50% nitrogen/50% carbon monoxide. The peaks identified by asterisks at 2327.2 cm<sup>-1</sup> in Figures 2 (top) and 3 and at 2138.4 cm<sup>-1</sup> in Figure 3 are the CARS signals from unshocked nitrogen and carbon monoxide, respectively. In the figures,  $P_0$  gives the pressure of the unshocked

(19) Maker, P. D.; Terhune, R. W. *Phys. Rev.* **1965**, *137*, A801–A818.

(20) Tolles, W. M.; Nibler, J. W.; McDonald, J. R.; Harvey, A. B. *Appl. Spectrosc.* **1977**, *31*, 253–272.

(21) Bloembergen, N. *Nonlinear Optics*; Benjamin: Reading, MA, 1965.

(22) Easley, G. L. *Coherent Raman Spectroscopy*; Pergamon: Oxford, 1981.

(23) Druet, S. A. J.; Taran, J.-P. E. *Prog. Quantum Electron* **1981**, *7*, 1–72.

(24) Roh, W. B.; Schreiber, P. W.; Taran, J.-P. E. *App. Phys. Lett.* **1976**, *29*, 174–176.

(25) Druet, S. A. J.; Attal, B.; Gustafson, T. K.; Taran, J.-P. E. *Phys. Rev. A* **1978**, *18*, 1529–1557.

(26) Bloembergen, N.; Lotem, H.; Lynch, R. T. *Indian J. Pure Appl. Phys.* **1978**, *16*, 151–158.

(15) Schmidt, S. C.; Moore, D. S.; Schiferl, D.; Châtelet, M.; Turner, T. P.; Shaner, J. W.; Shampine, D. L.; Holt, W. T. In *Advances in Chemical Reaction Dynamics*; Rentzepis, P. M., Capellos, C., Eds.; Reidel: Dordrecht, The Netherlands, 1986; pp 425–454.

(16) Moore, D. S.; Schmidt, S. C.; Shaw, M. S.; Johnson, J. D. *J. Chem. Phys.* **1989**, *90*, 1368–1376.

(17) Schmidt, S. C.; Moore, D. S.; Shaw, M. S.; Johnson, J. D. *J. Chem. Phys.* **1989**, *91*, 6765–6771.

(18) Moore, D. S.; Schmidt, S. C.; Shaw, M. S.; Johnson, J. D. *J. Chem. Phys.* **1991**, *95*, 5603–5608.

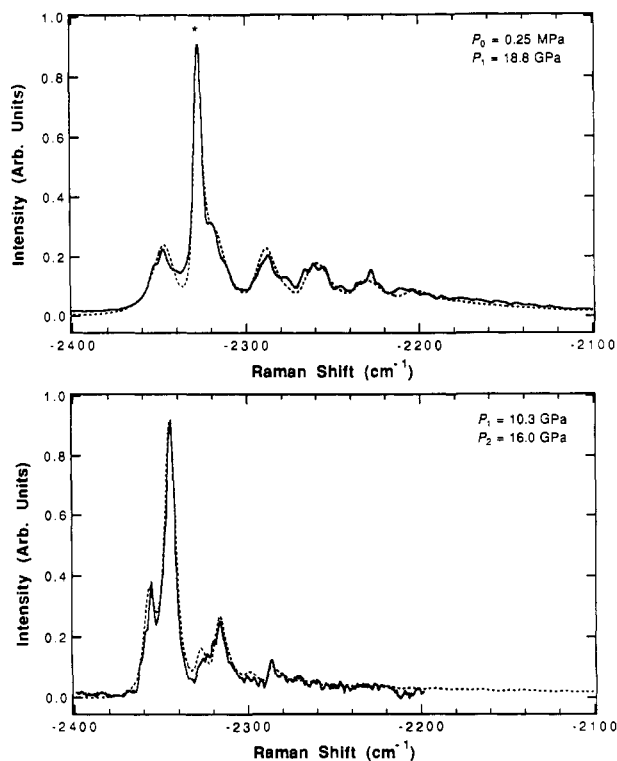


**Figure 2.** Samples of single-pulse, multichannel CARS spectra of nitrogen. Top: Spectra of unshocked and singly-shocked fluids obtained in an experiment in which the shock wave has not reached the window at the rear of the target assembly shown in Figure 1. Bottom: Spectra of singly- and doubly-shocked fluids obtained in an experiment in which the shock wave has been reflected from the rear window. Fluid pressures are denoted by  $P_0$  for unshocked fluid,  $P_1$  for singly-shocked fluid, and  $P_2$  for doubly-shocked fluid. The peak at  $2327.2 \text{ cm}^{-1}$  (identified by \*) is for unshocked nitrogen. Solid lines represent experimental data, and dashed lines correspond to calculated synthetic spectra.

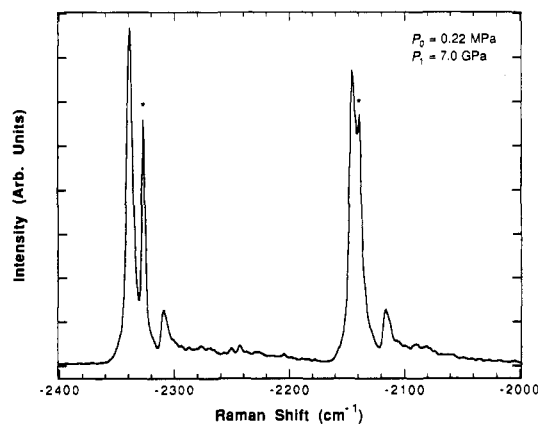


**Figure 3.** Single-pulse, multichannel CARS spectrum of a 50% nitrogen/50% carbon monoxide mixture. Fluid pressures are denoted by  $P_0$  for unshocked fluid and  $P_1$  for singly-shocked fluid. The peaks at  $2327.2$  and at  $2138.4 \text{ cm}^{-1}$  (both identified by \*) are for unshocked nitrogen and carbon monoxide, respectively. The solid line is the experimental result.

liquid. The remaining progression of lines in each figure is the fundamental transition and hot bands from singly-shocked fluid at pressure  $P_1$ .

If the shock wave reached and reflected from the rear window, both the singly- and doubly-shocked regions in the sample were interrogated by the incident laser beams. The resultant spectra, similar to those depicted by solid curves in Figure 2 (bottom), consisted of two partially overlapped progressions of transitions, each

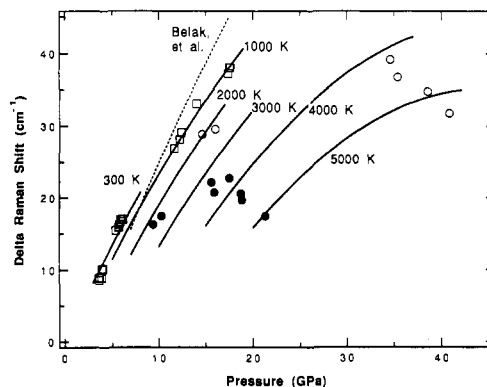


**Figure 4.**  $\Delta$  Raman shifts for the fundamental transition of nitrogen versus Hugoniot pressures achieved by shock compression (compared with  $2327.2 \text{ cm}^{-1}$ ). ●, CARS singly shocked; ○, CARS doubly shocked; □, spontaneous Raman scattering, diamond anvil cell; —, calculated isotherms; ---, Belak et al.<sup>10</sup>

progression arising from one of the interrogated regions. In the case shown, the nitrogen lines have not broadened sufficiently to obscure the individual peaks of the two progressions. In many cases the individual lines broaden sufficiently so that it is difficult to distinguish the singly-shocked from the doubly-shocked lines without spectral simulations. For these experiments,  $P_1$  is the pressure of the singly-shocked fluid and  $P_2$  is that of the doubly-shocked region.

We calculated the synthetic CARS spectra that represent the experimental data<sup>16-18</sup> using known techniques. In Figure 2, this result, after convolution with the appropriate slit function, is represented by the dashed line.

## Results

Figures 4-6 show the  $\Delta$  Raman shifts (the change of vibrational frequency from ambient) for the fundamental transitions of nitrogen,<sup>16,27</sup> oxygen,<sup>17</sup> and carbon monoxide<sup>18</sup> versus Hugoniot pressures achieved by shock compression.  $\Delta$  Raman shifts have been used so that the results for the different molecules can be readily compared. Similar results are also available for several hot-band transitions. Data are available to much higher pressures for nitrogen than for oxygen or carbon monoxide because both of the latter molecules become opaque when shocked to above 10 GPa. For oxygen, proximity- or collision-induced absorption is thought to cause the difficulty,<sup>17</sup> whereas for carbon monoxide, some form of chemical reaction is suspected.<sup>18</sup> The increase in nitrogen opacity above 20 GPa and above 40 GPa for the doubly-shocked fluid is thought to be the consequence of ionization.<sup>18</sup> Also given in Figure 4 are Raman scattering data obtained with static high-pressure methods.<sup>28</sup>

For all three molecules, the vibrational frequencies show a monotonic increase with increasing shock pressure. In the case of nitrogen, sufficiently large pressures are reached, so that the frequencies for both the singly- and doubly-shocked material appear to begin to decrease. Static high-pressure measurements of vibrational frequencies in solid nitrogen<sup>29,30</sup> and solid

(27) Schmidt, S. C.; Schiferl, D.; Zinn, A. S.; Ragan, D. D.; Moore, D. S. *J. Appl. Phys.* 1991, 69, 2793-2799.

(28) Zinn, A. S.; Schiferl, D.; Nicol, M. F. *J. Chem. Phys.* 1987, 87, 1267-1271.

(29) Reichlin, R.; Schiferl, D.; Martin, S.; Vanderborgh, C.; Mills, R. L. *Phys. Rev. Lett.* 1985, 55, 1464-1467.

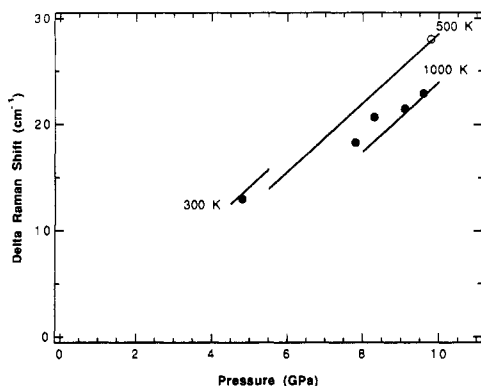


**Figure 5.**  $\Delta$  Raman shifts for the fundamental transition of oxygen versus Hugoniot pressure achieved by shock compression (compared with  $1551.3 \text{ cm}^{-1}$ ). ●, CARS singly shocked; ○, CARS doubly shocked; —, calculated isotherms.

hydrogen<sup>30</sup> show a similar reversal in the dependence of the Raman shift with increasing pressure. Initial explanations of this effect invoked a change in the molecular electronic structure at the highest densities.<sup>30</sup> Recent isotopic mixture studies indicate that the reversal in the frequency shift in the molecular solids at high density is most likely due to resonant interactions (that is, dynamic couplings may exist that would explain the reversal).<sup>31,32</sup> Although different possibilities have been suggested,<sup>33–36</sup> an explanation for this behavior of the vibrational frequencies is still being sought.

When the fluid is singly or doubly shocked to the same pressure, the difference in the measured  $\Delta$  Raman shifts noted in Figures 4–6 is related to the differences in temperature of the shocked materials. This difference is also observed for Raman scattering measurements of nitrogen made in the diamond anvil cell at equivalent pressures but lower temperatures. The effect of temperature on the potential functions and the portion of the potential sampled<sup>1</sup> manifests itself clearly by these differences in the vibrational frequencies. The advantage of using high-pressure experiments to separate the effects of pressure and temperature on dense fluid behavior has been previously noted.<sup>2</sup>

Because existing theoretical interpretations inadequately describe the results observed experimentally, a technique was needed to organize and compare the measurements. The measured Raman frequency shifts depicted in Figures 4–6 have been numerically fit to empirical relations of pressure and temperature.<sup>16,18,27</sup> The long curves in the figures show the positions of selected isotherms, obtained from the relevant empirical relation. Each isotherm is drawn over the approximate range of validity of the empirical fit. Also shown for comparison in Figure 4 are the nitrogen Raman fre-

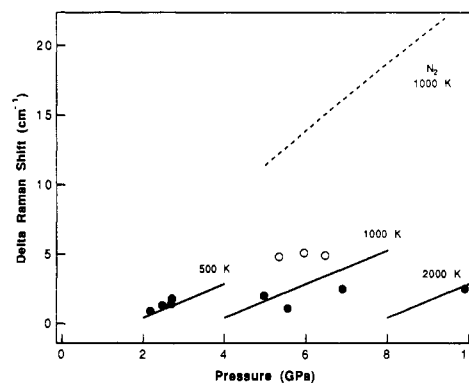


**Figure 6.**  $\Delta$  Raman shifts for the fundamental transition of carbon monoxide versus Hugoniot pressure achieved by shock compression (compared with  $2138.4 \text{ cm}^{-1}$ ). ●, CARS, single shock; ○, CARS, double shock; —, calculated isotherms; ---, calculated isotherm of nitrogen (compared with  $2327.2 \text{ cm}^{-1}$ ).

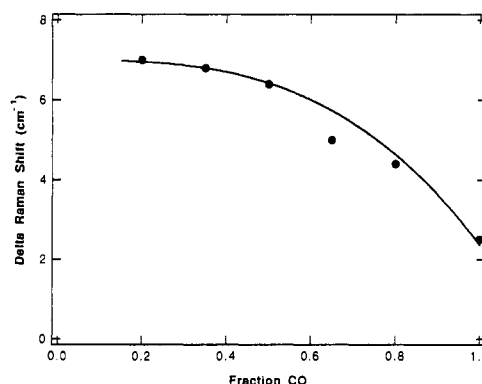


**Figure 7.**  $\Delta$  Raman shifts of CO compared with  $2138.4 \text{ cm}^{-1}$  versus fraction of CO in mixtures of  $\text{N}_2$  and CO at 7.2 GPa and  $\sim 1420 \text{ K}$ . The datum at 0.65 is near 6 GPa and is consequently slightly low compared with an empirical fit (—) of all of the CO and  $\text{N}_2$  data.<sup>16,18</sup>

quency shifts along a 2000 K isotherm from an approximation to Monte Carlo calculations by Belak, Eppers, and LeSar.<sup>10</sup> As pointed out by the authors,<sup>10</sup> the Monte Carlo calculations give frequencies that are slightly higher than experimental results, with the discrepancy becoming greater for increasing pressure. Possible reasons for this difference as briefly discussed in a previous publication<sup>16</sup> include dissociation and/or ionization. This discrepancy is being explored by LeSar.<sup>36</sup> No theoretical results are known for oxygen or carbon monoxide.

Comparison of the 1000 K isotherms for the three molecules shows that nitrogen and oxygen have similar shifts, with that of oxygen being slightly larger. However, the vibrational frequency shift with shock pressure for carbon monoxide is dramatically smaller than that observed for either nitrogen or oxygen. The 1000 K isotherm of nitrogen is drawn in Figure 6 along with the carbon monoxide results to emphasize this effect. This considerable difference is surprising in view of the fact that nitrogen and carbon monoxide are isoelectronic and have very similar properties such as liquid densities, boiling points, and shock Hugoniot up to 10 GPa.

Figure 7 shows preliminary results for the carbon monoxide vibrational frequency at 7.2 GPa and 1420 K versus the fraction of carbon monoxide in a carbon monoxide/nitrogen mixture. Note that, as the amount of carbon monoxide decreases, the measured vibrational frequency increases more rapidly near 100% carbon

(30) Bell, P. M.; Mao, H. K.; Hemley, R. J. *Physica B* 1986 139/140, 16–20.

(31) Schiferl, D.; LeSar, R.; Moore, D. S. In *Simple Molecular Systems at Very High Density*; Polian, A., Loubeyre, P., Boccara, N., Eds.; Plenum: New York, 1989; pp 303–328.

(32) Yu, Z. H.; Strachan, D.; Daniels, W. B. Manuscript in preparation.

(33) Nellis, W. J.; Holmes, N. C.; Mitchell, A. C.; van Thiel, M. *Phys. Rev. Lett.* 1984, 53, 1661–1664.

(34) Radousky, H. B.; Nellis, W. J.; Ross, M.; Hamilton, D. C.; Mitchell, A. C. *Phys. Rev. Lett.* 1986, 57, 2419–2422.

(35) Nellis, W. J.; Radousky, H. B.; Hamilton, D. C.; Mitchell, A. C.; Holmes, N. C.; Christianson, K. B.; van Thiel, M. *J. Chem. Phys.* 1991, 94, 2244–2257.

(36) LeSar, R. Private communication.

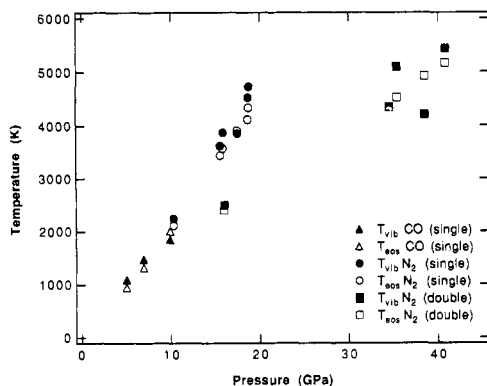


**Figure 8.** Equation-of-state temperatures  $T_{\text{eos}}$  and vibrational temperatures  $T_{\text{vib}}$  (extracted from the computed synthetic spectra) versus shock pressure for CO and  $\text{N}_2$ .

monoxide and less rapidly near 100% nitrogen. The nitrogen vibrational frequency exhibits a similar behavior, decreasing more rapidly near 100% nitrogen and less rapidly near 100% carbon monoxide. Clearly, this behavior of the vibrational frequencies is a manifestation of the influence that different molecular neighbors have on the intramolecular potentials. Previously, at much lower pressures and temperatures, the presence of a permanent dipole moment in carbon monoxide has been used to explain the much larger Raman line width in ambient liquid carbon monoxide versus nitrogen.<sup>37</sup> Other authors have noted the perturbation of vibrational frequencies and line broadening resulting from molecular interactions.<sup>38</sup> All of this evidence indicates that, if the intermolecular potential functions are to completely describe these high-density fluids, we must consider the detailed nature of the interacting molecules as well as many-body effects. An attempt to theoretically describe these observations is in progress.<sup>36</sup>

Experimental results<sup>39-43</sup> show that the vibrational relaxation time of the dense, fluid nitrogen decreases from several seconds at atmospheric pressure to approximately 0.2 ms at 0.3 GPa. Because these times are long, it was unclear whether at shock pressures and temperatures the relaxation time would decrease sufficiently rapidly (to <50 ns) to enable equilibration of the vibrational levels in the shock-compressed region interrogated by CARS. It was also unclear what effect impurities would have on the density dependence of the relaxation time.<sup>39,40</sup> For all experiments performed to date in which vibrational hot bands have appeared, the spectra are adequately represented by a simple model based on Boltzmann equilibrium of the vibrational levels.<sup>16,44</sup> This result implies that energy has been transferred from the bulk translational motion into the vibrational energy levels in a time less than or comparable to the characteristic time of the shock-compression experiment. For these experiments, this time is

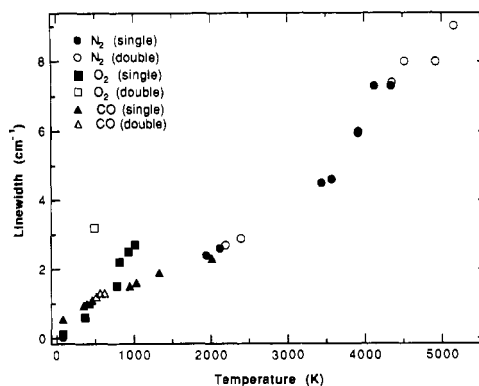


**Figure 9.** Raman line widths extracted from the synthetic spectral fits to fluid nitrogen, oxygen, and carbon monoxide CARS spectra plotted against shock temperatures.

less than 10 ns. For nitrogen this time represents a change of nearly 10 orders of magnitude from the ambient vibrational relaxation time of many seconds.

Because the vibrational populations appear to be in equilibrium, they can be used as a measure of the vibrational temperature. Figure 8 shows the calculated equation-of-state and vibrational temperatures versus shock pressures for both singly- and doubly-shocked  $\text{N}_2$  and singly-shocked CO. The reasonable agreement between the measured and calculated temperatures lends support to the model used to obtain the equation-of-state temperatures.<sup>8,9</sup>

In Figure 9, the Raman line widths<sup>16,18</sup> used to obtain the spectral fits of the shock-compressed fluid nitrogen, oxygen, and carbon monoxide spectra are presented versus temperature. The equation used to calculate the CARS spectra uses Lorentzian profiles to represent the spectral line shapes. Although this choice provides an adequate representation of our measured CARS spectra, it does not preclude the possibility of inhomogeneous broadening (that is, a Gaussian contribution to the line shapes). This effect would appear predominantly in the line wings, where our data are not accurate enough to distinguish between shapes. In addition, the limited signal/noise ratio does not permit the observation of line shape differences between the fundamental transition and the observed hot bands. Lorentzian profiles were chosen because they appeared to be a good first approximation far from the critical region.<sup>37,45</sup>

Two statements can be made about the spectral line width data. First, the vibrational dephasing time  $T_2$  has decreased from tens of picoseconds at liquid and near-critical densities<sup>45-48</sup> to a few picoseconds or less at shock pressures and temperatures. Collapse of the Q-branch from motional narrowing<sup>49-51</sup> is probably complete at the pressures and temperatures investigated here, and the line broadening probably results only from pure dephasing. (However, it must be noted that this notion may not be entirely correct because other lower density studies<sup>11</sup> have shown that vibra-

(37) Brueck, S. R. *J. Chem. Phys. Lett.* 1978, 53, 273-277.

(38) Akhmanov, S. A.; Gadjiev, F. N.; Koroteev, N. I.; Orlov, R. Yu.; Shumay, I. L. *Appl. Opt.* 1980, 19, 859-862.

(39) Manzanares, C.; Ewing, G. E. *J. Chem. Phys.* 1978, 69, 1418-1424.

(40) Chandler, D. W.; Ewing, G. E. *J. Chem. Phys.* 1980, 73, 4904-4913.

(41) Châtelet, M.; Kieffer, J.; Oksengorn, B. *Chem. Phys.* 1983, 79, 413-429.

(42) Châtelet, M.; Chesnoy, J. *Chem. Phys. Lett.* 1985, 122, 550-552.

(43) Khalil-Yahyavi, B.; Châtelet, M.; Oksengorn, B. *J. Chem. Phys.* 1988, 89, 3573-3578.

(44) Schmidt, S. C.; Moore, D. S.; Shaw, M. S. *Phys. Rev. B* 1987, 35, 493-496.

(45) Chesnoy, J. *Chem. Phys. Lett.* 1986, 125, 267-271.

(46) Chesnoy, J.; Weis, J. J. *J. Chem. Phys.* 1986, 84, 5378-5388.

(47) Kieffe, H.; Clouter, M. J.; Rich, N. H.; Ahmad, S. F. *Chem. Phys. Lett.* 1980, 70, 425-429.

(48) Clouter, M. J.; Kieffe, H. *J. Chem. Phys.* 1977, 66, 1737-1739.

(49) Temkin, S. I.; Burstein, A. I. *JETP Lett.* 1976, 24, 86-89.

(50) Brueck, S. R. *J. Chem. Phys. Lett.* 1977, 50, 516-520.

(51) Oksengorn, B.; Fabre, D.; Lavorel, B.; Saint-Loup, R.; Berger, H. *J. Chem. Phys.* 1991, 94, 1774-1784.

tional dephasing may not be separable from energy relaxation processes.)

The second statement to be made about Figure 9 is that, as the shock pressure increases along the shock Hugoniot, the spectral line widths for nitrogen, oxygen, and carbon monoxide appear to increase almost linearly with temperature. With the exception of the one doubly-shocked datum for oxygen, a significant dependence on density is not readily apparent. For example, the single- and double-shock data for nitrogen and carbon monoxide appear to fall on the same curve. Also, the nitrogen and carbon monoxide data seem to form a continuous line, suggesting another way in which these molecules are similar. Oxygen displays a different, but also nearly linear, line width dependence on the shock Hugoniot temperature. The steep repulsive core of the intermolecular potential is being sampled at the shock densities investigated here. Consequently, the change in density with increasing shock pressure is much less than the change in temperature. This fact, coupled with an observed weak density dependence of the line width,<sup>16</sup> could produce the results observed in Figure 9.

### Concluding Remarks

We are seeking a fundamental understanding of the detailed microscopic phenomenology of shock-induced chemical reaction and detonation waves by using pulsed, coherent anti-Stokes Raman scattering experiments to determine the vibrational frequencies and line widths in shock-compressed, high-pressure/high-temperature fluids. To date, we have confirmed that N<sub>2</sub>, O<sub>2</sub>, CO, N<sub>2</sub>O,<sup>52</sup> CH<sub>3</sub>NO<sub>2</sub>,<sup>15,53</sup> and C<sub>6</sub>H<sub>6</sub><sup>14</sup> still exist as

(52) Schmidt, S. C.; Moore, D. S. In *Proceedings of the International Symposium on Coherent Raman Spectroscopy*; Marowsky, G., Ed.; Springer-Verlag: Heidelberg, in press.

(53) Moore, D. S.; Schmidt, S. C. In *Proceedings of the Ninth Symposium (International) on Detonation*; Morat, W. J., Ed.; Naval Surface Warfare Center: Silver Spring, MD, 1989; Vol. I, pp 180-189.

molecules on the nanosecond to microsecond time scale behind the shock front and that energy is being transferred from the translational degrees of freedom into the vibrational modes. For N<sub>2</sub>, O<sub>2</sub>, and CO, the vibrational relaxation times decrease to less than a few nanoseconds in the shock-compressed state. For nitrogen, this difference represents a rate increase of nearly 10 orders of magnitude from ambient conditions. The vibrational population distribution appears to be Boltzmann and gives temperatures that agree satisfactorily with those obtained from equation-of-state calculations. Presently we are attempting to determine the vibrational temperatures of mixtures of these molecules.

We have experimentally shown the effect of the intermolecular potential (reflecting the thermodynamic environment of the shock-compressed state and many-body effects) on the intramolecular potential through vibrational frequency shift measurements. These results show differences in the behavior of N<sub>2</sub> and CO that have not been elucidated by shock Hugoniot data. We have used line width data, assuming homogeneous line broadening, to provide an estimate of dephasing times. For N<sub>2</sub>, O<sub>2</sub>, and CO, these times have decreased to a few picoseconds or less at the highest pressures studied. Future work will include efforts to elucidate the behavior of mixtures of diatomic fluids, to obtain the Raman spectra of triatomic molecular fluids, and to conduct isotopic exchange experiments at shock pressures and temperatures.

*The authors are grateful to the many fine people who have made these experiments possible and to J. D. Johnson, R. A. LeSar, D. Schiferl, and M. S. Shaw for many fruitful discussions. We thank A. Hartford and C. B. Storm for reading the manuscript, J. M. Neff for its preparation, and B. W. Burton for editing help. This work was supported by the U.S. Department of Energy.*

**Registry No.** N<sub>2</sub>, 7727-37-9; O<sub>2</sub>, 7782-44-7; CO, 630-08-0.